Cornel iridoid glycoside ameliorated Alzheimer's disease-like pathologies and necroptosis through RIPK1/MLKL pathway in young and aged SAMP8 mice

Denglei Ma
Xuanwu Hospital
Yanzheng Li
Xuanwu Hospital
Yanqiu Zhu
Xuanwu Hospital
Weipeng Wei
Xuanwu Hospital
Li Zhang
Xuanwu Hospital
Yali Li
Xuanwu Hospital
lin li (lilin@xwh.ccmu.edu.cn)
Xuanwu Hospital
Lan Zhang
Xuanwu Hospital

Research

Keywords: Aging, Alzheimer's disease, Senescence-accelerated mouse-prone 8 (SAMP8), Cornel iridoid glycoside, necroptosis

Posted Date: March 2nd, 2021

DOI: https://doi.org/10.21203/rs.3.rs-230305/v1

Abstract

Background

Aging is an important risk factor for sporadic Alzheimer's disease (AD) and other neurodegenerative diseases. Senescence-accelerated mouse-prone 8 (SAMP8) is used as an animal model for brain aging and sporadic AD researches. The aim of the current study was to investigate the pharmacological effects of cornel iridoid glycoside (CIG), an active ingredient of *Cornus officinalis*, on AD-type pathological changes in young and aged SAMP8 mice.

Methods

Nissl and immunohistochemical staining was applied to detect NeuN-labeled neurons and myelin basic protein-labeled myelin sheath,. Western blotting was used to detect the expression levels of related proteins of synapse, APP processing and necroptosis.

Results

The results showed that SAMP8 mice at the age of 6 and 14 months exhibited age-related neuronal loss, demyelination, synaptic damage, and APP amyloidogenic processing. In addition, the increased levels of receptor-interacting protein kinase-1 (RIPK1), mixed lineage kinase domain-like protein (MLKL) and p-MLKL indicating necroptosis were found in the brain of SAMP8 mice. Intragastric administration of CIG for 2 months alleviated neuronal loss and demyelination, increased the expression of synaptophysin, postsynaptic density protein 95 and AMPA receptor subunit 1, elevated the levels of soluble APPα fragment and a disintegrin and metalloproteinase 10 (ADAM10), and decreased the levels of RIPK1, p-MLKL and MLKL in the brain of young and aged SAMP8 mice.

Conclusion

This study denoted that CIG might be a potential drug for aging-associated neurodegenerative diseases such as AD.

Introduction

Aging is closely related to decline of learning and memory, with a higher incidence of neurodegenerative diseases, including sporadic AD (Guerreiro and Bras, 2015; Lardenoije et al., 2018). Senescence-accelerated mouse prone 8 (SAMP8) is a mouse stain with accelerated senescence status, developed from AKR/J series (Takeda, 1999), and has been used as an animal model for brain aging and AD (Cheng et al., 2014). Numerous articles have demonstrated that SAMP8 mice display advancing aging status and share common characteristics with the aged and AD patients, including age-related deteriorative

cognition and behavioral alteration (Chen et al., 2004; Cheng et al., 2014), neuropathological phenotypes such as neuron loss and synaptic plasticity impairment (Li et al., 2013; Lin et al., 2014), hyperphosphorylation of tau forming neurofibrillary tangles (Canudas et al., 2005), APP amyloidogenic processing (Dong et al., 2015), and other pathological features in age-related neurodegeneration (Akiguchi et al., 2017). Senescence-accelerated mouse-resistant 1 (SAMR1) exhibits normal phenotypes, and is used as non-age accelerated control of SAMP8 mice (Butterfield and Poon, 2005).

Cornus officinalis Sieb. et Zucc is a traditional herbal medicine and widely applied to treat age-related diseases and dementia in China. Cornel iridoid glycoside (CIG) is the main effective ingredient of *Cornus officinalis*. Morroniside and loganin are the major components of CIG. It has been reported that morroniside and loganin exhibit the antioxidative (Wang et al., 2009), antiosteoporosis (Li et al., 2010), and inhibiting cholinesterase and β-secretase activities (Bhakta et al., 2016) *in vitro*, as well as antidiabetic effect *in vivo* (Yokozawa et al., 2010). In our previous studies, CIG showed protective pharmacological effects against focal cerebral ischemia (Yao et al., 2009; Ya et al., 2010) and traumatic brain injury by inhibiting inflammation and apoptosis (Ma et al., 2018). We recently found that CIG suppressed tau hyperphosphorylation and aggregation through activating protein phosphatase 2A in a P301L mutant tau transgenic mouse model (Ma et al., 2019b; Ma et al., 2020).

As aging is one of the key risk factors of AD, we studied the pharmacological effects of CIG using SAMP8 mice. In our previous article, we found SAMP8 mice showed cognitive impairments and senescent status, and CIG treatment reversed these changes at different ages (Ma et al., 2016). However, the effects and mechanisms of CIG on the AD pathologies on SAMP8 mice remains unclear.

Necroptosis is a form of programmed necrotic cell death caused by many micro-environmental factors (Christofferson and Yuan, 2010). Recent studies found that necroptosis is involved in the normal aging and several neurodegenerative disorders, such as AD (Caccamo et al., 2017; Li et al., 2017; Deepa et al., 2018). Whether necroptosis plays a role in the pathologies in SAMP8 mice and the intervention effects of CIG remains unclear. In the current study, we investigated the effects of CIG on neuronal loss, demyelination, synaptic damage, APP amyloidogenic processing, and necroptosis in the brain of young and aged SAMP8 mice.

Methods

2.1. Drugs

Cornel iridoid glycoside (CIG) was extracted from the sarcocarp of *Cornus officinalis* Sieb. et Zucc as described in our previous paper (Yao et al., 2009). *Cornus officinalis* Sieb. et Zucc was purchased from Beijing Tongrentang Company (Beijing, China). Morroniside accounted for 67% and loganin 33%. As oxiracetam has been approved as a nootropic agent to treat patients with AD clinically (Rozzini et al., 1993), oxiracetam was used as a positive control drug in the present study.

2.2. Animals

Male SAMP8 and SAMR1 mice were obtained from First Affiliated Hospital, Tianjin University of Traditional Chinese Medicine (Tianjin, China). All mice were housed under a normal light-dark (12 h/12 h) cycle and standard temperature conditions (22 ± 2°C), with free access to food and clean water. All mice were habituated for 7 days before starting the experiment.

2.3. Animal grouping and treatment

Two different ages of SAMR1/SAMP8 mice were applied and allocated to two experiment tranches as previously reported (Ma et al., 2016). (1) Young SAMP8 mice at 4-month-old received treatments of three doses CIG (50, 100, 200 mg/kg/d), saline (as model group) or oxiracetam (as positive control drug, 360 mg/kg/d) for 2 months; same age SAMR1 mice were treated with saline or 100 mg/kg/d CIG; n = 15 per group. (2) Aged SAMP8 mice at 12-month-old received saline (n = 18) or CIG (200 mg/kg/d; n = 15); SAMR1 mice (n = 12) received normal saline for 2 months.

The dosages of CIG were chosen based on our previous studies in mice (Ma et al., 2016), and the dosage of oxiracetam was converted from human clinical dosage. CIG and oxiracetam were dissolved in normal saline, intragastrically administered to mice once a day, and lasted for 2 months.

2.4. Tissue collection

For immunohistochemical analysis, mice were perfused transcardially with 4% paraformaldehyde after being anesthetized by intraperitoneal injection of 1.25% Avertin (0.2 ml/10 g body weight) (Sigma, USA). The brain was removed, post-fixed and then dehydrated in 15 ~ 30% sucrose/0.1 M PBS. Brain tissues were cut into series horizontal sections with 30 μm thick in a cryostat slicer after being frozen in isopentane (620E, Thermo fisher Scientific, USA).

For western blotting, brain tissues (4 mice per group) were homogenized in lysis buffer (50 mM Tris–HCl, 0.1% SDS, 150 mM NaCl, 1% Nonidet P-40, 2 mM EGTA, 0.5% sodium deoxycholate) with phosphatase/protease inhibitor cocktail (Thermo fisher Scientific, USA). Homogenates were centrifuged at 12,000 g for 20 min at 4°C. Supernatants were collected and boiled for 5 min. Consequently, RC-DC Protein Assay Kit (Bio-Rad Laboratories, USA) was applied to determine protein concentrations.

2.5. Nissl and Immunohistochemical staining

For Nissl staining, dehydrated brain sections were stained with 0.1% cresyl violet acetate (Sigma-Aldrich, St. Louis, MO, USA) for 20 min, rinsed in distilled water three times (2 min), differentiated in 95% ethanol with acetic acid (1 min), dehydrated with alcohol and cover-slipped with neutral balsam (ZSGB-bio, Beijing, China).

Three brain slices in each mouse were applied for immunohistochemical staining of NeuN and MBP. Endogenous peroxidase activity was blocked by exposing to 3% H_2O_2 for 15 min, and then sealed in 10% serum at 37°C for 1 h. The sections were then incubated with the primary antibodies (Table 1) at 4°C. After being washed, sections were then incubated with goat anti-rabbit/mouse non-Biotin detection system

(PV9002/9001, Zsbio, Beijing, China), and immune complexes were visualized by a DAB substrate kit (Zsbio, Beijing, China).

Table 1
Primary antibodies used in this study.

Antibody	Type	Species	Dilution	Company	Catalog	Use
NeuN	Mono-	M	1:200	Millipore	MAB377	IHC
MBP	Mono-	Rat	1:200	Millipore	MAB386	IHC
Synaptophysin	Poly-	R	1:1000	Sigma	SAB4502906	WB
PSD95	Poly-	R	1:1000	CST	3409	WB
GluR1	Poly-	R	1:1000	Abcam	ab31232	WB
GAPDH	Mono-	R	1:1000	CST	5174	WB
APP	Mono-	R	1:1000	CST	5174	WB
sAPPα	Poly-	R	1:1000	Covance	SIG-39139	WB
ADAM10	Poly-	R	1:1000	Sigma	A2726	WB
BACE-1	Poly-	R	1:1000	Abcam	ab2077	WB
RIPK1	Mono-	R	1:1000	CST	3493	WB
p-MLKL(Ser345)	Mono -	R	1:1000	CST	37333	WB
MLKL	Mono -	R	1:1000	CST	37705	WB
Mono-, monoclonal; Poly-, polyclonal; M, mouse; R, rabbit;IHC, Immunohistochemistry; WB, western blotting.						
Figures and legends						

Pictures were photographed under Olympus microscope, and analyzed using Image-Pro plus 5.0 software (Media Cybernetics, Inc., Bethesda, USA). For comparison of the number of neurons between groups, signals were extracted from images by using the color threshold function with identical settings in Image-Pro plus 5.0 software. Three slices per mouse were analyzed to get an average value. Quantification of the number of neurons was achieved and analyzed by experimenter blinded to the groups.

2.6. Western blotting

Proteins were loaded and separated on 10% SDS-PAGE gel, and transferred onto polyvinylidene fluoride (PVDF) membranes (Millipore, USA). Membranes were then blocked by 5% non-fat milk in TBST buffer (Tris-buffered Saline-Tween 20, consisting of 10 mM Tris–HCl, 100 mM NaCl, and 0.05% Tween-20), and incubated with primary antibodies (see Table 1). On the second day, after incubation with ahorseradish peroxidase-conjugated anti-rabbit or anti-mouse IgG secondary antibody (1:2000, Cell Signaling

Technology, USA), immune complex was detected by ECL detection reagent for Western blotting (Immobilon™ Western Chemiluminescent HRP Substrate, Millipore, USA). Band intensity was analyzed using TINA (Raytest Isotopenme Bgerate 190 GmbH, Straubenhardt, Germany).

2.7. Statistical analysis

All data were provided as mean ± SEM (standard error of mean). Data were analyzed using one-way ANOVA followed by Tukey's post hoc test to determine statistical significance among groups. $P < 0.05$ was regarded as statistically significant. Graphs were plotted in Prism version 5.0 software (GraphPad Software Inc., USA).

Results

CIG alleviated neurons loss and demyelination in the brain of young and aged SAMP8 mice

The neurons in the brain of mice were detected by NeuN immunohistochemical staining. The results indicated a notable loss of neurons in the cerebral cortex of SAMP8 at the ages of 6 and 14 months compared with age-matched control SAMR1 mice ($P < 0.01$, $P < 0.05$). Intragastric administration of CIG and Oxiracetam for 2 months significantly increased the number of neurons in the cerebral cortex of young and aged SAMP8 mice ($P < 0.01$, $P < 0.05$; Fig. 1).

Myelin basic protein (MBP), the main protein of the myelin sheath, is used to represent mature oligodendrocyte and the integrity of myelin. In the present study, the immunohistochemistry results showed that the expression of MBP was evidently declined in the corpus callosum of young and aged SAMP8 rats ($P < 0.05$; Fig. 2). However, treatment with CIG (100 and 200mg/kg) significantly elevated the expression of MBP in young and aged SAMP8 mice ($P < 0.05$; Fig. 2). These results demonstrated that CIG reduced demyelination of young and aged SAMP8 mice.

CIG increased the expression of synaptic-related proteins in the hippocampus of young and aged SAMP8 mice

The normal integration of synaptic proteins and glutamate receptors at the synapse determines the synaptic plasticity, which is closely associated with cognitive functions (Harris and Littleton, 2015). Synaptophysin is a pre-synaptic protein, and postsynaptic density protein 95 (PSD95) mainly expressed in post synaptic area (Kwon and Chapman, 2011). In the present study, western blotting results showed that the expression of synaptophysin decreased in the hippocampus of young and aged SAMP8 model mice compared with SAMR1 ($P < 0.05$, $P < 0.01$). CIG and Oxiracetam treatment significantly elevated the levels of synaptophysin in young SAMP8 mice ($P < 0.05$; Fig. 3). Moreover, the expression of PSD95 declined in the hippocampus of aged SAMP8 model mice compared with SAMR1 ($P < 0.05$); CIG treatment significantly increased the levels of PSD95 in young SAMP8 mice ($P < 0.05$; Fig. 3).

GluR1, a subunit of α-amino-3-hydroxy-5-methyl-4-isoxazolepropionic acid receptors (AMPA) receptor, plays important roles in synaptic transmissions and long-term potentiation (LTP) (Reisel et al., 2002). In the present study, western blotting results showed GluR1 expression obviously decreased in the hippocampus of aged SAMP8 model mice compared with SAMR1 control group ($P < 0.05$); CIG treatment significantly increased the levels of GluR1 in young and aged SAMP8 mice ($P < 0.05$; Fig. 3).

CIG promoted APP non-amyloidogenic processing in the cerebral cortex of SAMP8 mice at different ages

β-amyloid precursor protein (APP) can be cleaved by ADAM10 (α-secretase) and release a neuroprotective fragment, which is considered as APP non-amyloidogenic processing (Marcello et al., 2017). In the current study, SAMP8 model mice showed lower protein levels of ADAM10 at 6 and 14 months of age ($P < 0.05$) and sAPPα at 14 months of age in the cerebral cortex compared with SAMR1 control group ($P < 0.05$, Fig. 5). CIG treatment evidently increased the levels of ADAM10 and sAPPα in young SAMP8 mice ($P < 0.05$), and also significantly elevated the level of sAPPα in aged SAMP8 mice ($P < 0.05$; Fig. 4). Oxiracetam obviously elevated the expression of ADAM10 and sAPPα in young SAMP8 mice ($P < 0.05$; Fig. 4). There was no significant difference in the expression levels of full-length APP and BACE-1 among all groups of young and aged SAMP8 mice (Fig. 4).

CIG inhibited RIPK1/MLKL pathway in the cerebral cortex of SAMP8 mice

Receptor-interacting protein kinase-1 (RIPK1) and mixed lineage kinase domain-like protein (MLKL) are the key elements that mediate necroptosis (Caccamo et al., 2017). In the present study, we detected the changes of RIPK1 and MLKL in the brain of SAMP8 mice using western blotting. The results showed that the expression of RIPK1 markedly increased in the cerebral cortex of young and aged SAMP8 model mice compared with SAMR1 control mice ($P < 0.01$), and CIG treatment evidently decreased the level of RIPK1 in young and aged SAMP8 mice ($P < 0.05$; Fig. 5). Moreover, the expression of phosphorylated and total MLKL increased obviously in the cerebral cortex of SAMP8 model mice ($P < 0.01$, $P < 0.05$). CIG treatment significantly reduced the levels of phosphorylated MLKL in the cerebral cortex of young SAMP8 mice ($P < 0.05$), and total MLKL in young and aged SAMP8 mice ($P < 0.05$; Fig. 5). Oxiracetam markedly decreased the expression of phosphorylated MLKL in young SAMP8 mice ($P < 0.05$; Fig. 5).

Discussion

The present study revealed that CIG treatment effectively ameliorated neuronal loss and demyelination, increased synaptic proteins (synaptophysin, PSD95 and GluR1) in the cerebral cortex and hippocampus of both young and aged SAMP8 mice. Meanwhile, CIG also increased the APP non-amyloidogenic processing by increasing sAPPα and ADAM10. Moreover, CIG inhibited necroptosis through down-regulating RIPK1/MLKL pathway. As a positive control drug, Oxiracetam increased the expression of MBP, synaptophysin, ADAM10 and sAPPα, and decreased the level of phosphorylated MLKL in the brain of

SAMP8 at 6 months of age. Compared with Oxiracetam, CIG showed better effects on ameliorating AD-related pathologies.

From the age of 6 months onward, SAMP8 mice exhibit obvious and age-related Aβ deposition, a major pathogenesis and pathology of AD (Dong et al., 2015). Pathogenic Aβ fragment is generated through amyloidogenic pathways of APP processing by β-secretase (BACE1) and γ-secretase. In healthy brain, the major proteolytic way of APP is processed by α-secretase (ADAM10), which produces a soluble and nontoxic APP fragment (sAPPα) and a C-terminal fragment (Lammich et al., 1999). Consistent with former studies (Huang et al., 2014; Katayama et al., 2016), we found decreased levels of ADAM10 and sAPPα in the brain of SAMP8 mice at the ages of 6 and 14 months. Several studies have found that active compounds decrease brain Aβ accumulation and prolonged survival in SAMP8 mice via increasing the expression of ADAM10 (Kitaoka et al., 2013; Katayama et al., 2016). In the current study, CIG treatment obviously increased expression levels of ADAM10 and sAPPα in the brain of SAMP8 mice at 6 and 14 months of age, indicating CIG may inhibit the Aβ production via activating the non-amyloidogenic processing of APP.

Synapse is the basic element involved in normal neuronal interactions in the brain, and synaptic plasticity is the biological basis of learning and memory (Harris and Littleton, 2015). In synapse, α-amino-3-hydroxy-5-methyl-4-isoxazolepropionic acid receptors (AMPARs) belong to glutamate receptors involved in many forms of synaptic plasticity (including LTP) and excitatory neurotransmissions in the hippocampus (Diering and Huganir, 2018).Propagation of toxic proteins (such as Aβ and phosphorylated tau) through synapse and synaptic dysfunction appear to be important contributors to cognitive impairments, and therapies targeting these deficits show the potential to improve cognition in AD (Spires-Jones and Hyman, 2014; Rajmohan and Reddy, 2017). Consistent with previous studies (Lin et al., 2014), we found obvious synaptic loss and decreased expression of synaptophysin, PSD-95 and GluR1 in the hippocampus of young and aged SAMP8 mice. CIG treatment significantly reversed these changes, suggesting that CIG may protect the normal synaptic transmission and cognitive impairment in SAMP8 mice.

RIPK1 and necroptosis are activated in AD brain, and positively correlated with Braak stage, and inversely correlated with brain weight and cognitive scores (Caccamo et al., 2017; Ofengeim et al., 2017). Lowering necroptosis activation by inhibiting RIPK1 were reported to reduce cell loss in a mouse model of AD (Caccamo et al., 2017). RIPK1 is a key molecule to initiate necroptosis, and interacts with RIPK3 into complex IIb (Zelic et al., 2018). And MLKL, a pseudo-kinase, would be phosphorylated and inserted into the plasma membrane as oligomers, leading to the initiation of necroptosis (Cai et al., 2014; Chen et al., 2014). In current study, expression levels of RIPK1, phosphorylated and total MLKL were increased, indicating the activated necroptosis in the brain of young and aged SAMP8 mice. Treatment with CIG evidently reversed these changes in SAMP8 mice. It is suggested that CIG may inhibit the activation of RIP1/MLKL pathway and necroptosis, which may explain CIG's protective effects on neuronal loss in the brain of SAMP8 mice.

Earlier interventions plays an important role in delaying the onset of Alzheimer's dementia (Crous-Bou et al., 2017). The learning and memory ability of SAMP8 mouse strain is impaired as early as 4 months of age, and the average lifespan of SAMP8 mice is 12–14months old (Flood and Morley, 1992; Lin et al., 2014). In our study, we used two tranches of SAMP8 mice at 4- and 12-month-old age to represent the different stages of AD, and investigated the effects of CIG intervention over different phases. In our previous article, CIG improved cognitive impairments in SAMP8 mice at earlier phases (Ma et al., 2016). In the present article, CIG showed better effects on APP non-amyloidogenic processing, synaptic plasticity and necroptosis at earlier stages, which may explain the effects of earlier intervention on cognitive impairments. Through our research on the different intervention effects of CIG on SAMP8 mice, we proposed a suggestion that earlier treatment of CIG might benefit the patients of AD or mild cognitive impairments (MCI).

Conclusion

In conclusion, the current study demonstrated that two-month treatment of CIG alleviated neuronal loss, demyelination and enhanced synaptic transmission via increasing the levels of synaptophysin, PSD95 and GluR1 in the brain of SAMP8 mice at 6 and 14 months. Moreover, CIG promoted the APP non-amyloidogenic processing through increasing ADAM10 (α-secretase) and sAPPα. Additionally, CIG inhibited necroptosis through down-regulating RIPK1/MLKL pathway in the brain of SAMP8 mice. It is suggested that CIG may be a potential drug for aging-related neurodegenerative diseases such as AD. And earlier treatment of CIG might show better effects on improving pathological changes and cognitive impairments for patients of AD or MCI.

Declarations

Ethics approval and consent to participate

Animal experimental procedures were approved by Bioethics Committee of Xuanwu Hospital, Capital Medical University.

Consent for publication

Not applicable.

Availability of data and material

Please contact corresponding authors for data requests.

Competing interests

The authors declare that they have no competing interests.

Funding

This research was supported by National Natural Science Foundation of China (81473373, 81874351, 81673406); Capital Science and Technology Leading Talent Training Project (Z191100006119017), and Beijing Hospitals Authority Ascent Plan (DFL20190803).

Acknowledgements

Not applicable.

Authors' contributions

This study was designed by Denglei Ma, Lin Li and Lan Zhang. Animal experiment was conducted by Yanqiu Zhu and Yanzheng Li. Li Zhang, Weipeng Wei and Yali Li performed western blotting and immunohistochemistry. Denglei Ma, Lin Li and Lan Zhang analyzed the data and drafted the manuscript. All authors read and approved the final manuscript.

References

Akiguchi, I., Pallàs, M., Budka, H., et al., 2017. SAMP8 mice as a neuropathological model of accelerated brain aging and dementia: Toshio Takeda's legacy and future directions. Neuropathology 37 (4), 293-305.

Bhakta, H.K., Park, C.H., Yokozawa, T., Min, B., Jung, H.A., Choi, J.S., 2016. Kinetics and molecular docking studies of loganin, morroniside and 7-O-galloyl-d-sedoheptulose derived from Corni fructus as cholinesterase and β-secretase 1 inhibitors. Arch. Pharm. Res. 39(6), 794-805.

Butterfield, D.A., Poon, H.F., 2005. The senescence-accelerated prone mouse (SAMP8): A model of age-related cognitive decline with relevance to alterations of the gene expression and protein abnormalities in Alzheimer's disease. Exp. Gerontol. 40(10), 774-783.

Caccamo, A., Branca, C., Piras, I.S., et al., 2017. Necroptosis activation in Alzheimer's disease. Nat. Neurosci. 20, 1236-1246.

Cai, Z., Jitkaew, S., Zhao, J., et al., 2014. Plasma membrane translocation of trimerized MLKL protein is required for TNF-induced necroptosis. Nat. Cell Biol. 16(1), 55-65.

Canudas, A.M., Gutierrez-Cuesta, J., Rodriguez, M.I., et al., 2005. Hyperphosphorylation of microtubule-associated protein tau in senescence-accelerated mouse (SAM). Mech. Ageing Dev. 126(12), 1300-1304.

Chen, G.H., Wang, Y.J., Wang, X.M., Zhou, J.N., 2004. Accelerated senescence prone mouse-8 shows early onset of deficits in spatial learning and memory in the radial six-arm water maze. Physiol. Behav. 82(5), 883-890.

Chen, X., Li, W., Ren, J., et al., 2014. Translocation of mixed lineage kinase domain-like protein to plasma membrane leads to necrotic cell death. Cell Res. 24(1), 105-121.

Cheng, X., Zhou, W., Zhang, Y., 2014. The behavioral, pathological and therapeutic features of the senescence-accelerated mouse prone 8 strain as an Alzheimer's disease animal model. Ageing Res. Rev. 13, 13-37.

Christofferson, D.E., Yuan, J., 2010. Necroptosis as an alternative form of programmed cell death. Curr. Opin. Cell Biol. 22(2), 263-268.

Crous-Bou, M., Minguillon, C., Gramunt, N., et al. 2017. Alzheimer's disease prevention: from risk factors to early intervention. Alzheimers Res. Ther. 9, 71.

Deepa, S.S., Unnikrishnan, A., Matyi, S., Hadad, N., Richardson, A., 2018. Necroptosis increases with age and is reduced by dietary restriction. Aging Cell 17(4), e12770.

Diering, G.H., Huganir, R.L., 2018. The AMPA receptor Code of synaptic plasticity. Neuron 100(2), 314-329.

Dong, W., Wang, F., Chen, Y., et al., 2015. Electroacupuncture reduces Aβ production and BACE1 expression in SAMP8 mice. Front. Aging Neurosci. 7, 148.

Flood, J.F., and Morley, J.E. 1992. Early onset of age-related impairment of aversive and appetitive learning in the SAM-P/8 mouse. J Gerontol 47, B52-9.

Guerreiro, R., Bras, J., 2015. The age factor in Alzheimer's disease. Genome Med. 7, 106.

Harris, K.P., Littleton, J.T., 2015. Transmission, development, and plasticity of synapses. Genetics 201(2), 345-375.

Huang, J., Wu, D., Wang, J., et al., 2014. Effects of Panax notoginseng saponin on α, β, and γ secretase involved in Aβ deposition in SAMP8 mice. Neuroreport 25(2), 89-93.

Katayama, S., Sugiyama, H., Kushimoto, S., Uchiyama, Y., Hirano, M., Nakamura, S., 2016. Effects of sesaminol feeding on brain Abeta accumulation in a senescence-accelerated mouse-prone 8. J. Agric. Food Chem. 64(24), 4908-4913.

Kitaoka, K., Shimizu, N., Ono, K., et al., 2013. The retinoic acid receptor agonist Am80 increases hippocampal ADAM10 in aged SAMP8 mice. Neuropharmacology 72, 58-65.

Kwon, S.E., Chapman, E.R., 2011. Synaptophysin regulates the kinetics of synaptic vesicle endocytosis in central neurons. Neuron 70(5), 847-54.

Lammich, S., Kojro, E., Postina, R., et al., 1999. Constitutive and regulated alpha-secretase cleavage of Alzheimer's amyloid precursor protein by a disintegrin metalloprotease. Proc. Natl. Acad. Sci. U. S. A. 96(7), 3922-3927.

Lardenoije, R., Pishva, E., Lunnon, K., van den Hove, D.L., 2018. Neuroepigenetics of Aging and Age-Related Neurodegenerative Disorders. Prog. Mol. Biol. Transl. Sci. 158, 49-82.

Lee, H.K., Takamiya, K., Han, J.S., et al., 2003. Phosphorylation of the AMPA receptor GluR1 subunit is required for synaptic plasticity and retention of spatial memory. Cell 112(5), 631-643.

Li, D., Meng, L., Xu, T., et al., 2017. RIPK1-RIPK3-MLKL-dependent necrosis promotes the aging of mouse male reproductive system. eLife 6, e27692.

Li, G., Cheng, H., Zhang, X., et al., 2013. Hippocampal neuron loss is correlated with cognitive deficits in SAMP8 mice. Neurol. Sci. 34(6), 963-969.

Li, M., Wang, W., Wang, P., Yang, K., Sun, H., Wang, X., 2010. The pharmacological effects of morroniside and loganin isolated from Liuweidihuang Wan, on MC3T3-E1 cells. Molecules 15(10), 7403-7414.

Lin, N., Pan, X., Chen, A., et al., 2014. Tripchlorolide improves age-associated cognitive deficits by reversing hippocampal synaptic plasticity impairment and NMDA receptor dysfunction in SAMP8 mice. Behav. Brain Res. 258, 8-18.

Ma, D., Luo, Y., Huang, R., et al., 2019. Cornel iridoid glycoside suppresses tau hyperphosphorylation and aggregation in a mouse model of tauopathy through increasing activity of PP2A. Curr. Alzheimer Res. 16(14), 1316 - 1331.

Ma, D., Wang, N., Fan, X., et al. 2018. Protective effects of cornel iridoid glycoside in rats after traumatic brain injury. Neurochem. Res. 43(4), 959-971.

Ma, D., Zhu, Y., Li, Y., et al. 2016. Beneficial effects of cornel iridoid glycoside on behavioral impairment and senescence status in SAMP8 mice at different ages. Behav. Brain Res. 312, 20-29.

Ma, D., Luo, Y., Huang, R., et al. 2020. Cornel iridoid glycoside suppresses hyperactivity phenotype in rTg4510 mice through reducing tau pathology and improving synaptic dysfunction. Current Medical Science 40, 1031-1039.

Marcello, E., Borroni, B., Pelucchi, S., Gardoni, F., Di Luca, M., 2017. ADAM10 as a therapeutic target for brain diseases: from developmental disorders to Alzheimer's disease. Expert Opin. Ther. Targets 21(11), 1017-1026.

Ofengeim, D., Mazzitelli, S., Ito, Y., et al., 2017. RIPK1 mediates a disease-associated microglial response in Alzheimer's disease. Proc. Natl. Acad. Sci. U. S. A. 114, E8788-E8797.

Rajmohan, R., Reddy, P.H., 2017. Amyloid-Beta and phosphorylated Tau accumulations cause abnormalities at synapses of Alzheimer's disease neurons. J. Alzheimers Dis. 57(4), 975-999.

Reisel, D., Bannerman, D.M., Schmitt, W.B., et al., 2002. Spatial memory dissociations in mice lacking GluR1. Nat. Neurosci. 5, 868-873.

Spires-Jones, T.L., Hyman, B.T., 2014. The intersection of amyloid beta and tau at synapses in Alzheimer's disease. Neuron 82(4), 756-771.

Takeda, T., 1999. Senescence-accelerated mouse (SAM): a biogerontological resource in aging research. Neurobiol. Aging 20(2), 105-110.

Wang, W., Sun, F.L., An, Y., et al., 2009. Morroniside protects human neuroblastoma SH-SY5Y cells against hydrogen peroxide-induced cytotoxicity. Eur. J. Pharmacol. 613(1-3), 19-23.

Ya, B.L., Li, C.Y., Zhang, L., Wang, W., Li, L., 2010. Cornel iridoid glycoside inhibits inflammation and apoptosis in brains of rats with focal cerebral ischemia. Neurochem. Res. 35, 773-781.

Yao, R.Q., Zhang, L., Wang, W., Li, L., 2009. Cornel iridoid glycoside promotes neurogenesis and angiogenesis and improves neurological function after focal cerebral ischemia in rats. Brain Res. Bull. 79(1), 69-76.

Yokozawa, T., Kang, K.S., Park, C.H., et al., 2010. Bioactive constituents of Corni Fructus: The therapeutic use of morroniside, loganin, and 7-O-galloyl-D-sedoheptulose as renoprotective agents in type 2 diabetes. Drug Discov. Ther. 4(4), 223-234.

Zelic, M., Roderick, J.E., O Donnell, J.A., et al., 2018. RIP kinase 1-dependent endothelial necroptosis underlies system ic inflammatory response syndrome. J. Clin. Invest. 128(5), 2064-2075.

Zhao, L.H., Ding, Y.X., Zhang, L., Li, L., 2010. Cornel iridoid glycoside improves memory ability and promotes neuronal survival in fimbria-fornix transected rats. Eur. J. Pharmacol. 647(1-3), 68-74.

Figures

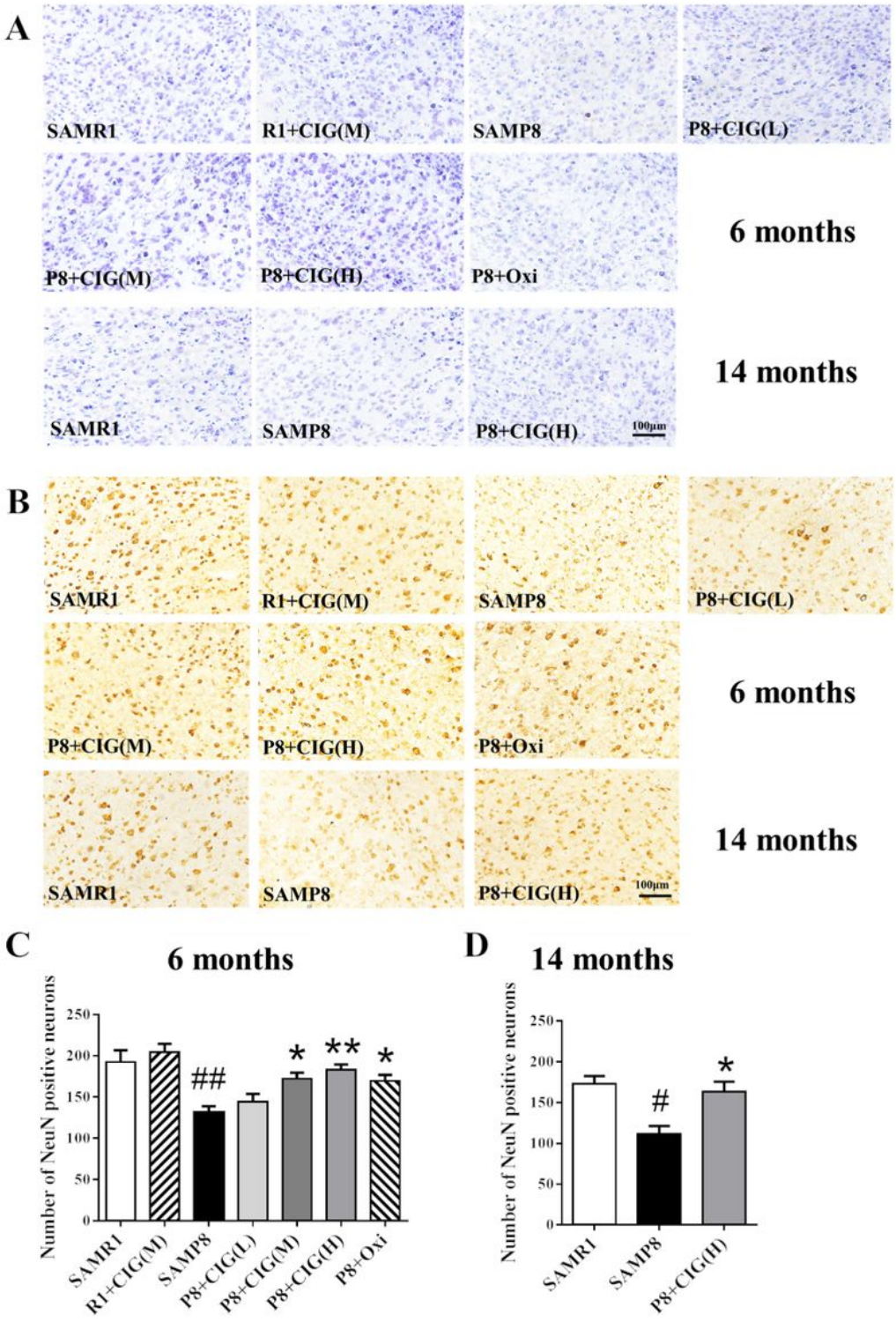

Figure 1

Effects of CIG on neuronal loss in the cerebral cortex of SAMP8 mice at young and aged SAMP8 mice. (A) Representative images of Nissl staining in the cerebral cortex of mice at 6 and 14 months of age; (B) Representative images of immunohistochemical staining for NeuN-labelled neurons in the cerebral cortex of mice at 6 and 14 months of age; scale bar = 100 μm. (C) Quantitative analysis of the number of NeuN-labelled neurons in the cerebral cortex of mice at 6 months of age, (D) at 14 months of age. Data are

expressed as the mean ± SEM, n = 3 each group. #P<0.05, ##P<0.01, SAMP8 model group vs SAMR1 control group; *P<0.05, **P<0.01, drug-treated SAMP8 groups vs SAMP8 model group. SAMR1, senescence accelerated mouse/resistant 1; R1+ CIG (M), SAMP8 mice treated with CIG at 100mg/kg; SAMP8, senescence accelerated mouse/prone 8; P8+CIG (L), SAMP8 mice treated with CIG at 50 mg/kg; P8+CIG (M), SAMP8 mice treated with CIG at 100mg/kg; P8+CIG (L), SAMP8 mice treated with CIG at 200 mg/kg; P8+Oxi, SAMP8 mice treated with oxiracetam at 360 mg/kg; NeuN; neuronal nuclei antigen.

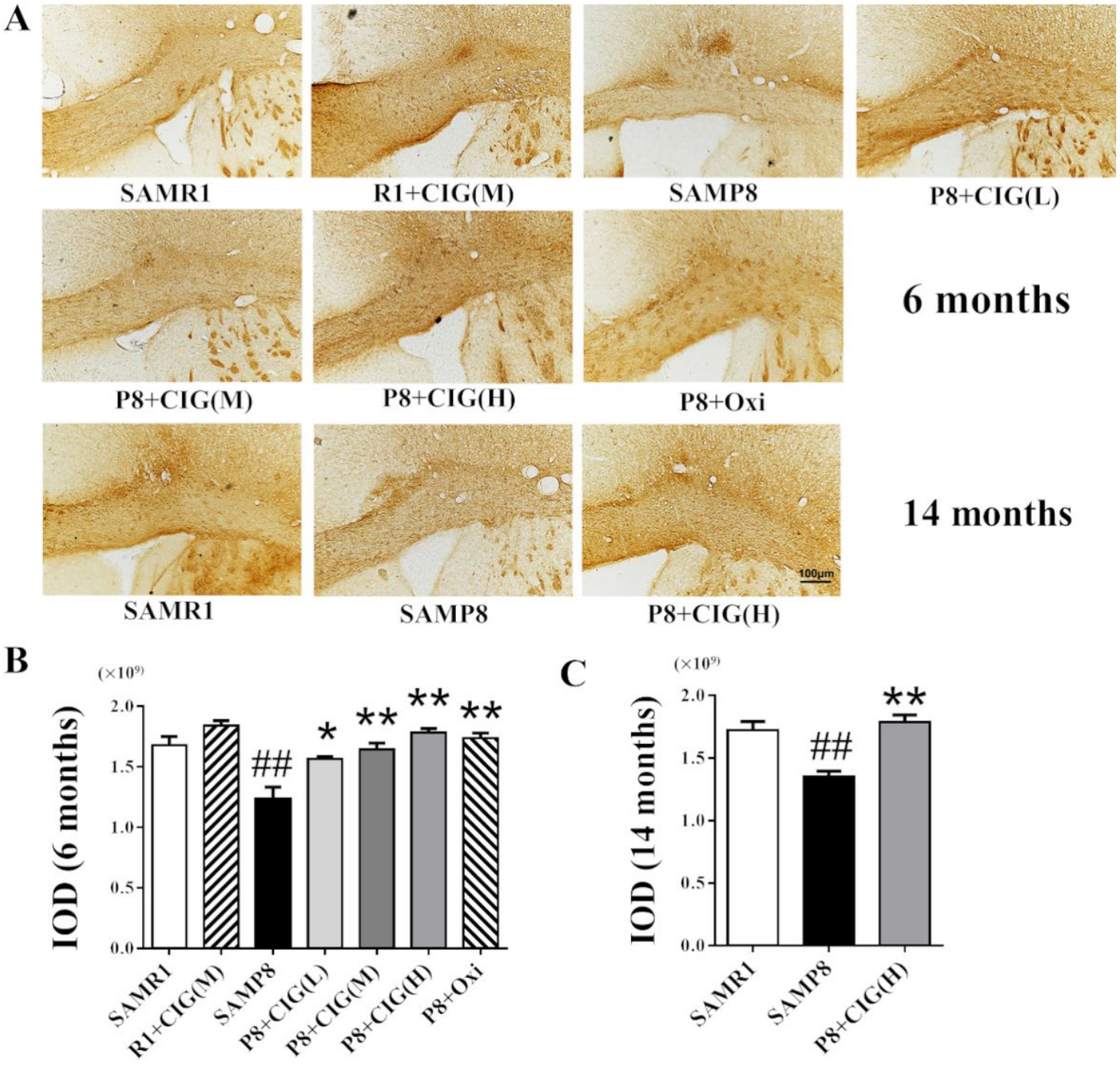

Figure 2

Effects of CIG on demyelination in the corpus callosum of SAMP8 mice at young and aged SAMP8 mice. (A) Representative images of myelin basic protein (MBP) immunohistochemistry in the corpus callosum of SAMP8 mice at young and aged SAMP8 mice; scale bar = 100 μm. (B) Quantitative analysis of integrated optical density (IOD) for MBP immunohistochemistry at 6 months of age, (D) at 14 months of age. Data are expressed as the mean ± SEM, n = 3 each group. #P<0.05, ##P<0.01, SAMP8 model group vs SAMR1 control group; *P<0.05, **P<0.01, drug-treated SAMP8 groups vs SAMP8 model group. IOD, integrated optical density.

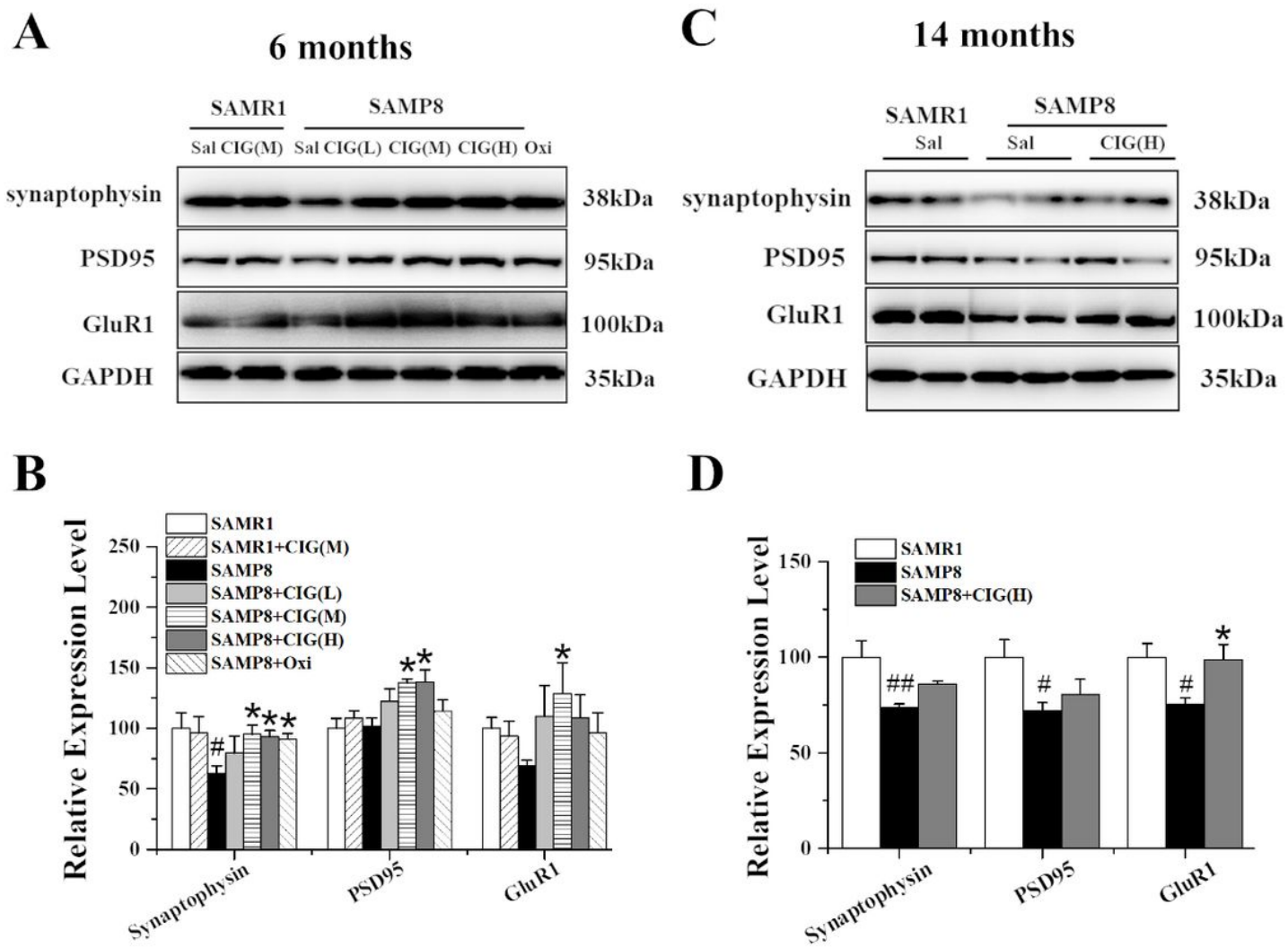

Figure 3

Effects of CIG on the expression of synaptic plasticity-related proteins in the hippocampus of young and aged SAMP8 mice (Western blotting). (A, B) Representative images and quantitative analysis of the expression of synaptophysin, PSD95, GluR1 in the hippocampus of mice at 6 months of age. (C, D) at 14 months of age. GAPDH served as an internal loading control and the relative intensity in the SAMR1 control group was set as 100%. Data are expressed as the mean ± SEM, n = 4 each group. #P<0.05, ##P<0.01, SAMP8 model group vs SAMR1 control group; *P<0.05, **P<0.01, drug-treated SAMP8 groups

vs SAMP8 model group. Sal, normal saline (vehicle); PSD95, postsynaptic density protein 95; GluR1, AMPA receptor subunit 1.

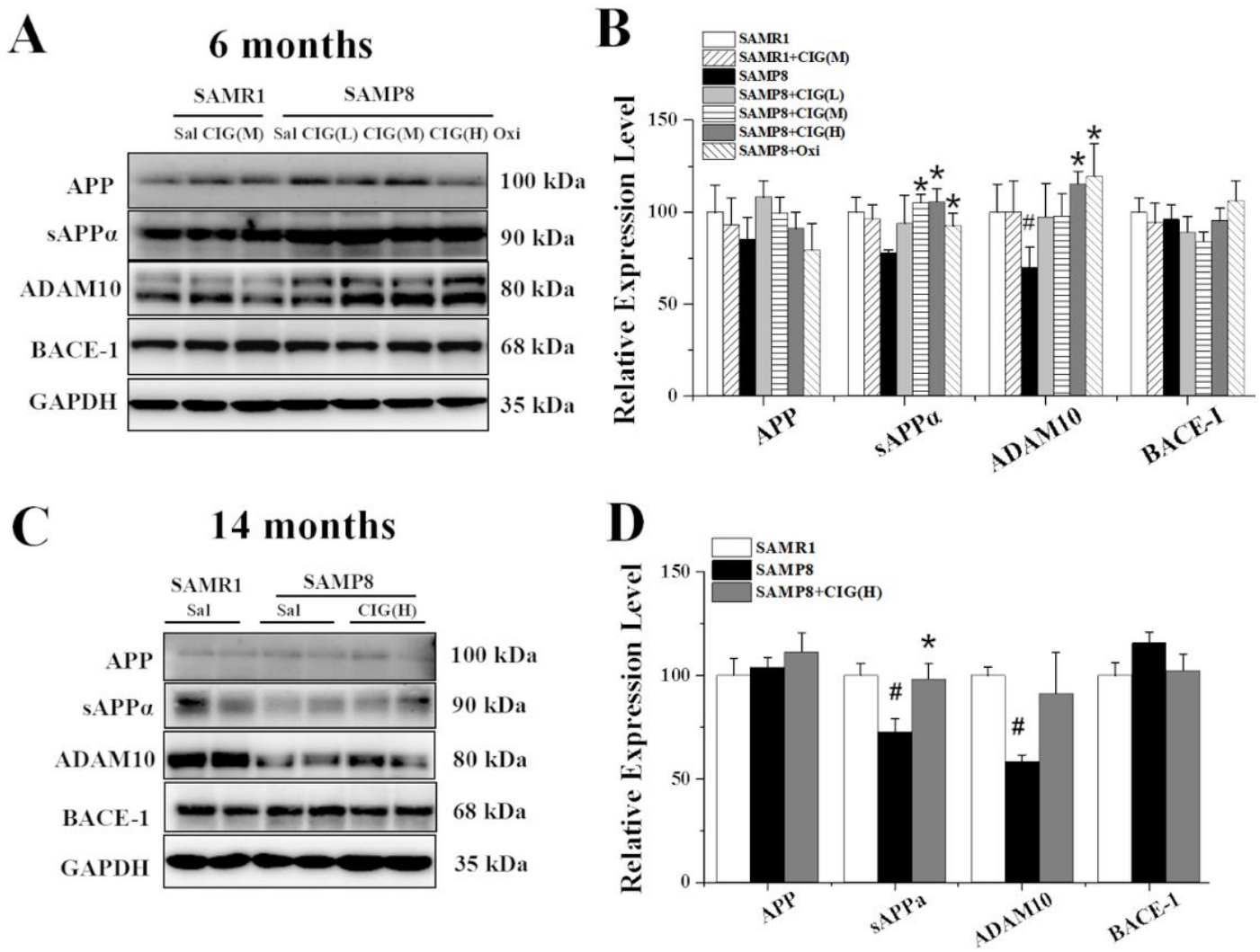

Figure 4

Effects of CIG on the expression of APP-related proteins in the cerebral cortex of SAMP8 mice at different ages (Western blotting). (A, B) Representative images and quantitative analysis of the expression of APP, sAPPα, ADAM10 and BACE-1 in the cerebral cortex of mice at 6 months of age. (C, D) at 14 months of age. GAPDH served as an internal loading control and the relative intensity in the SAMR1 control group was set as 100%. Data are expressed as the mean ± SEM, n = 4 each group. #P<0.05, ##P<0.01, SAMP8 model group vs SAMR1 control group; *P<0.05, **P<0.01, drug-treated SAMP8 groups vs SAMP8 model group. APP, β-amyloid precursor protein; sAPPα, soluble APPα fragment; ADAM10, a disintegrin and metalloproteinase 10 (α-secretase); BACE-1, β-site APP cleaving enzyme (β-secretase).

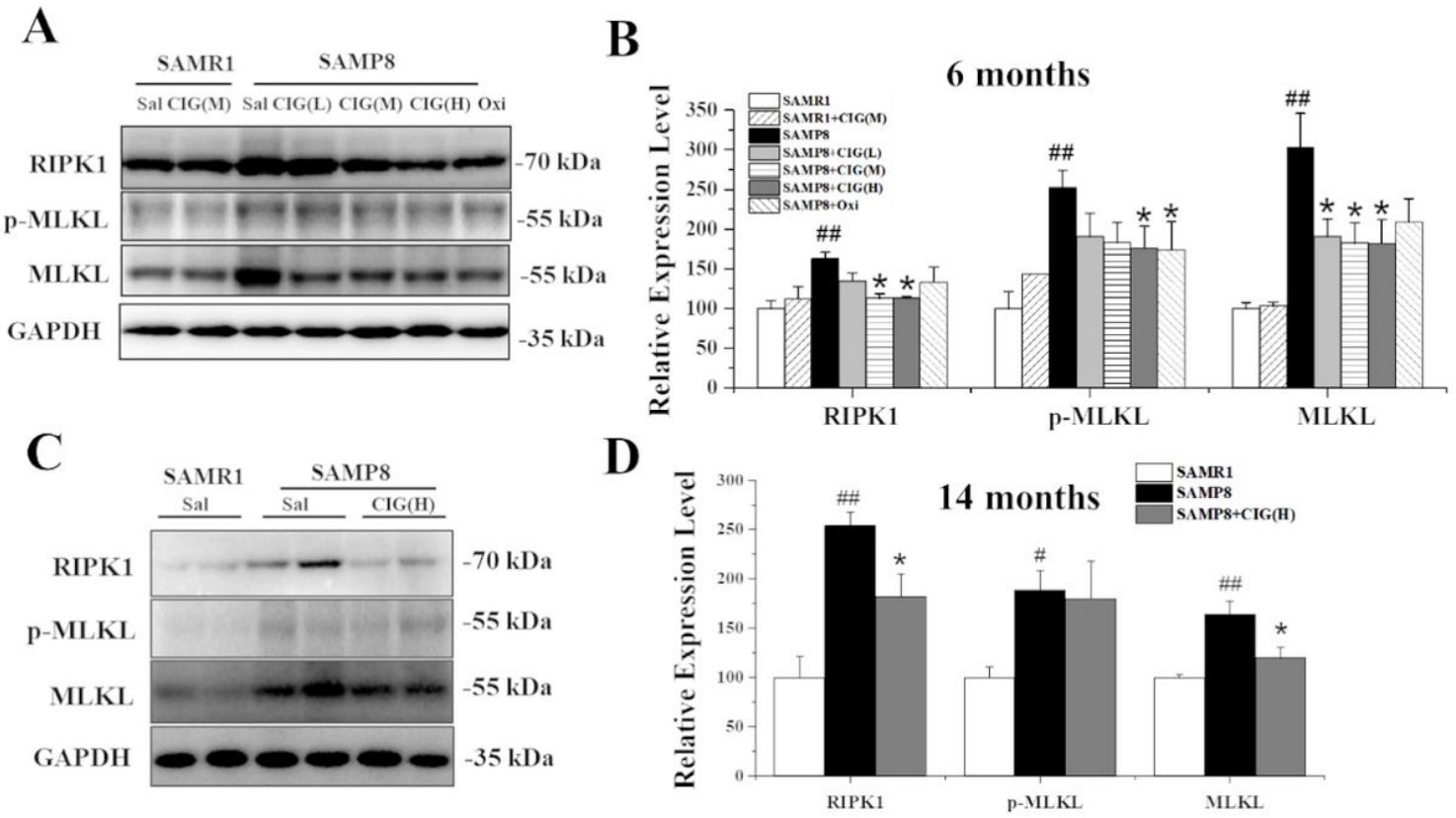

Figure 5

Effects of CIG on RIPK1/MLKL pathway in the cerebral cortex of young and aged SAMP8 mice (Western blotting). (A, B) Representative images and quantitative analysis of the expression of RIPK1, phosphorylated MLKL and total MLKL in the cerebral cortex of mice at 6 months of age. (C, D) at 14 months of age. GAPDH served as an internal loading control and the relative intensity in the SAMR1 control group was set as 100%. Data are expressed as the mean ± SEM, n = 4 each group. #P<0.05, ##P<0.0: SAMP8 model group vs SAMR1 control group; *P<0.05, **P<0.01: drug-treated SAMP8 groups vs SAMP8 model group. RIPK1, receptor-interacting protein kinase-1; MLKL, mixed lineage kinase domain-like protein; p-MLKL, phosphorylated MLKL at Ser345.